



Original Article

# Cilostazol Promotes Angiogenesis and Increases Cell Proliferation After Myocardial Ischemia–Reperfusion Injury Through a cAMP-Dependent Mechanism

JIANGJIN LI <sup>1</sup>, XIAOLI XIANG,<sup>2</sup> HAI XU,<sup>1</sup> and YAFEI SHI<sup>1</sup>

<sup>1</sup>Department of Cardiology, The Affiliated Huaian No.1 People's Hospital of Nanjing Medical University, Huai'an 223300, Jiangsu, China; and <sup>2</sup>Department of Nephrology, The Affiliated Huaian No.1 People's Hospital of Nanjing Medical University, Huai'an 223300, Jiangsu, China

(Received 12 December 2018; accepted 4 October 2019; published online 17 October 2019)

Associate Editor Kristyn Simcha Masters oversaw the review of this article.

## Abstract

**Purpose**—Previous study indicated the protective role of cilostazol in ischemia–reperfusion (I/R) injury. Here, we aimed to explore the function of cilostazol in myocardial I/R injury and the underlying mechanism.

**Methods**—The myocardial I/R injury rat model was constructed, and the expression levels of vascular endothelial growth factor (VEGF), hepatocyte growth factor (HGF), basic fibroblast growth factor (bFGF), platelet-derived growth factor receptor b (PDGF-B) and the number of new blood vessels were measured by qRT-PCR and immunohistochemistry. VSMC and HUVEC cells were treated with hypoxia to induce *in vivo* I/R injury model. The protein expression of AKT, endothelial nitric oxide synthase (eNOS) and apoptosis-related protein levels were detected by western blotting. Besides, the positive staining rate and cell viability were tested by 5-bromo-2-deoxyuridine (BrdU)/4',6-diamidino-2-phenylindole (DAPI) or DAPI/TdT-mediated dUTP Nick-End Labeling (TUNEL) staining and MTT assay.

**Results**—Cilostazol promoted angiogenesis by increasing the number of new blood vessels and up-regulating the expression of VEGF, HGF, bFGF and PDGF-B in myocardial I/R-injury rat model. The *in vitro* experiments showed that cilostazol increased the level of eNOS and AKT, and also enhanced cell proliferation in hypoxia-treated VSMC and HUVEC cells. Furthermore, after 8-Br-cAMP treatment, VEGF, HGF, bFGF, PDGF-B, p-AKT and p-eNOS expression were up-regulated, while cleaved-caspase 3 and cleaved-PARP expression were down-regulated. In addition, the effects of cilostazol on cell viability and apoptosis were

aggravated by 8-Br-cAMP and attenuated after KT-5720 treatment.

**Conclusion**—Cilostazol could promote angiogenesis, increase cell viability and inhibit cell apoptosis, consequently protecting myocardial tissues against I/R-injury through activating cAMP.

**Keywords**—Cilostazol, Ischemia–reperfusion injury, Myocardium, cAMP, Angiogenesis.

## INTRODUCTION

The morbidity and mortality of ischemic heart diseases are constantly increasing over time and extremely harmful to human health.<sup>8</sup> The prevention of cardiac dysfunction and protection of ischemic myocardium are mainly through timely reconstruction of coronary blood transport, including thrombolysis, coronary artery bypass grafting (CABG) and percutaneous coronary intervention (PCI).<sup>23</sup> However, these therapies may lead to reperfusion injury, thrombosis or stenosis of patients.<sup>13,17</sup> Therefore, it has become a major issue in cardiology, and it is necessary to explore mechanism underlying cardiac ischemia–reperfusion (I/R) injury and look for effective methods to alleviate myocardial damage.<sup>24</sup>

Cilostazol (CAS#: 73963-72-1), chemically known as 6-[4-(1-cyclohexyl-5-tetrazole) butoxy]-1, 2, 3, 4-tetrahydro-2-oxoquinoline, has the abilities of vasodilation and anti-platelet aggregation.<sup>20,31</sup> It mainly increases the concentration of cyclic adenosine monophosphate (cAMP) or releases adenosine diphosphate (ADP) and 5-hydroxytryptamine (5-HT)

Address correspondence to Jiangjin Li, Department of Cardiology, The Affiliated Huaian No.1 People's Hospital of Nanjing Medical University, Huai'an 223300, Jiangsu, China. Electronic mail: Lijiangjinlsl@163.com

by inhibiting the activity of phosphodiesterase (PDE) in platelets and vascular smooth muscle or the production of thromboxane A<sub>2</sub> (TXA<sub>2</sub>) in the phospholipid membranes.<sup>37</sup> Some studies have found that cilostazol could reduce serum triglycerides (TG) and increase high-density lipoprotein (HDL) to lower cardiovascular risk.<sup>32</sup> Kariyazono *et al.* and Hayward *et al.* believed that cilostazol could inhibit the initial, secondary aggregation and release of platelets induced by ADP, adrenaline, collagen and arachidonic acid, and had anti-thrombotic effects on the models of cerebral circulation and peripheral circulatory disorders.<sup>11,18</sup> Besides, cilostazol also exerts effective effects in preventing of ischemic stroke and bleeding events.<sup>15</sup> Therefore, cilostazol can commonly be used to treat atherosclerosis, arteritis and chronic arterial occlusion caused by diabetes, and is especially suitable for patients who are resistant to aspirin.<sup>2,15,19</sup>

Importantly, despite the anti-thrombotic and vasodilating effects of cilostazol, is reported to protect against I/R-induced injury in various tissues or cells, such as hepatocytes, skeletal muscle and cerebral I/R model.<sup>3,10,33</sup> However, the role of cilostazol in myocardial I/R-injury is still unclear. Therefore, to study the potential protective effects of cilostazol in myocardial I/R-injury and explore the underlying mechanism, we established myocardial I/R rat model and *in vitro* cell models. The results showed that cilostazol promoted angiogenesis and increases cell proliferation through a cAMP-dependent mechanism, thereby alleviating pathological damage of myocardial I/R.

## MATERIALS AND METHODS

### *I/R Injury Rat Model and Tissue Collection*

Male Sprague–Dawley (SD) rats (n = 40) weighing 250–280 g were purchased from the Animal Center of Guangdong Medical Laboratory (Guangzhou, China). The rats were randomly divided into four groups (n = 10): sham group, sham + cilostazol group, I/R group and I/R + cilostazol group. Rats in the sham + cilostazol and I/R + cilostazol group were intragastrically administered at a dose of 20 mg/kg/day of cilostazol (HY-17464; MedChemExpress, New Jersey, USA) for 7 days prior to I/R surgeries,<sup>35</sup> and rats in sham and I/R group were given an equal amount of distilled water. The dose of cilostazol in rats was counted according to the equivalent dose formula (EDF) of cilostazol between animals and human body, and the formula was as follow:  $D_m = D_h (K_m/K_h) (W_h/W_m)^{1/3}$ .<sup>16</sup> After fasting overnight, rats were anesthetized with 10% chloral hydrate (0.36 mL/100 g;

Maclin Inc., Shanghai, China). Subsequently, the left anterior descending coronary artery of rat was isolated and threaded after thoracotomy. I/R injury rat models were established by ligation for 30 min and loosening for 120 min. After successful establishing I/R injury rat model, rats were immediately received cilostazol (30 mg/kg) or the same amount of normal saline once. After 72 h of reperfusion, part of the myocardial tissue in the I/R-injured area was cut and embedded after freezing. Tissue sections were air-dried and fixed in acetone at room temperature for 30 min. All experimental procedures and protocols were followed by the Institutional Animal Ethics Committee of the Affiliated Huaian No.1 People's Hospital of Nanjing Medical University. Ethical Guidelines were approved by the Ethical Committee of the Affiliated Huaian No.1 People's Hospital of Nanjing Medical University.

### *Myocardial Infarct Size Assay*

Collected tissues were added into 6-well plates containing 2,3,5-triphenyltetrazole chloride (TCC, Solarbio, Beijing, China) at 37 °C for 20 min in the dark, washed in the tissue flushing solution (Solarbio, Beijing, China) and then the color change of tissues was observed and photographed. Non-infarct area stained red and infarct area was grayish white in the tissues.

### *Hematoxylin–Eosin (HE) Staining*

Tissues were embedded in paraffin, stained in hematoxylin staining solution (Beyotime, Shanghai, China) for 15 min, added eosin staining solution (Beyotime, Shanghai, China) for 4 min and dehydrated in ethanol. Dried tissues were observed and photographed using a microscope (Leica Microsystems, Weitzlar, Germany).

### *Immunohistochemistry*

After immersing in xylene, absolute ethanol, 95% ethanol and 75% ethanol (all from Solarbio, Beijing, China), tissue sections were blocked with 10% goat serum blocking solution (Solarbio, Beijing, China) for 30 min at room temperature, and rabbit anti-human von willbrand factor (vWF) antibody (Bioss Biotech Inc., Beijing, China) was added and incubated at 4 °C overnight. Subsequently, tissues were incubated in secondary antibody (Bioss Biotech Inc., Beijing, China) at 37 °C for 25 min, washed twice by phosphate buffer saline (PBS; Solarbio, Beijing, China) for 5 min, stained in diaminobenzidine (DBA) and hematoxylin (Solarbio, Beijing, China) for 5 min, and then observed

and photographed under a microscope (Leica Microsystems, Weitzlar, Germany).

#### *Hypoxia-Induced (H/I) Cell Model*

Human vascular smooth muscle cell (VSMC) (CRL-1999) and vascular endothelial cell (HUVEC) (CRL-1730) were purchased from ATCC (Manassas, USA), and cultured in Kaighn's modification of Ham's F-12 (F12K) medium (Gibco, California, USA) containing 15% fetal bovine serum (FBS; Sigma-Aldrich, St. Louis, USA) at 37 °C. The cells were randomly divided into 6 groups: control group, control + cilostazol group, H/I group, H/I + cilostazol group, H/I + cilostazol + 8-Br-cAMP and H/I + cilostazol + KT-5720 group.

The cultured cells in H/I groups were replaced with F12K medium containing 5% FBS overnight at 37 °C. Then, cells were washed in phosphate buffered saline (PBS) and changed high-purity N<sub>2</sub>-saturated F12K medium and incubated in a constant temperature incubator at 37 °C after being filled with 92% N<sub>2</sub>, 3% O<sub>2</sub> and 5% CO<sub>2</sub> for 12 h. Then, all cells were replaced with Serum-free low sugar F12K medium at 37 °C in an incubator with 95% O<sub>2</sub> and 5% CO<sub>2</sub> for 4 h. In addition, cilostazol (10 μM), 8-Br-cAMP (100 μM, cAMP analogue, Abcam Inc., Shanghai, China) and KT-5720 (1 μM, cAMP antagonist, Abcam Inc., Shanghai, China) were added to the medium before hypoxia treatment, respectively.

#### *Western Blotting*

The cells were lysed using 100 μL of pre-chilled RIPA lysate (Millipore, Billerica, USA), and the total protein concentration was tested using ultraviolet (UV) spectrophotometer (Aucy Instrument Inc., Shanghai, China). Total protein (40 μL/well) was added and transferred to membranes for 1 h. Rabbit monoclonal or polyclonal antibodies of vascular endothelial growth factor (VEGF; ab32152), hepatocyte growth factor (HGF; ab83760), basic fibroblast growth factor (bFGF; ab8880), platelet-derived growth factor receptor b (PDGF-B; ab23914), protein kinase B (AKT; ab8805), phosphorylated AKT (ab38449), endothelial nitric oxide synthase (eNOS; ab5589), phosphorylated eNOS (ab184154), cleaved-caspase-3 (ab32042), caspase-3 (ab13847), poly ADP-ribose polymerase (PARP; ab74290), cleaved-PARP (ab32064) and β-catin (ab124964; all 1:500) were obtained from Abcam Inc. (Shanghai, China), added to membranes and incubated at 4 °C overnight. After washing with PBS, horseradish peroxidase-labeled goat anti-rabbit IgG (ab6721, 1:1000; Abcam Inc. Shanghai, China) was added and incubated for 2 h at room

temperature. A gel imaging system (Bio-Rad, Hercules, USA) collected the chemiluminescent substrate image on the polyvinylidene fluoride (PDVF) membrane.

#### *Quantitative Real Time Polymerase Chain Reaction (qRT-PCR)*

The total RNA was extracted using Beyozol with chloroform (Beyotime, Shanghai, China), mixed with Vortex-5 (Qilinbeier Inc., Haimen, China) and placed at room temperature for 2–3 min. The precipitate after centrifugation was washed repeatedly with 75% pre-chilled ethanol and re-dissolved with diethyl pyrocarbonate (DEPC; Beyotime, Shanghai, China). 5 μL RNA was reversely transcribed into cDNA using BeyoRT™ II M-MLV reverse transcriptase (Beyotime, Shanghai, China). The reaction solution was subjected to agarose gel electrophoresis, and the optical density value of the experimental strip was detected by image software (NIH Image, Bethesda, USA) and calculated by 2<sup>-ΔΔCt</sup> method.<sup>1</sup>

#### *Cell Proliferation Assay*

Cell proliferation assay was tested using 5-bromo-2-deoxyuridine (BrdU)/4',6-diamidino-2-phenylindole (DAPI) double staining. The cells were digested with 0.25% trypsin (Thermo Fisher Scientific, Waltham, USA) and added Brdu (MedChemExpress, New Jersey, USA) until cell fusion. The fused cells were fixed with 4% paraformaldehyde (Thermo Fisher Scientific, Waltham, USA) for 30 min, denatured with 2 N hydrogen chloride (Thermo Fisher Scientific, Waltham, USA) for 30 min at room temperature, blocked with 1:20 goat serum (Solarbio, Beijing, China) for 20 min, and incubated with anti-BrdU primary antibody (ab1983, 1:200; Abcam Inc. Shanghai, China) and goat anti-mouse IgG (ab6785, Abcam Inc. Shanghai, China) in a humidified incubator at 4 °C for 45 min. The cells were finally counterstained with DAPI (Beyotime, Shanghai, China) and observed under a fluorescence microscope (Leica Microsystems, Weitzlar, Germany).

#### *Cell Apoptosis Assay*

Cell apoptosis assay was assessed by using DAPI/TdT-mediated dUTP Nick-End Labeling (TUNEL) double staining. The prepared cells were fixed with 4% paraformaldehyde (Thermo Fisher Scientific, Waltham, USA) for 30 min, treated with 0.3% Triton X-100 (Solarbio, Beijing, China) for 5 min, stained with DAPI (1 g/L; Beyotime, Shanghai, China) diluted 1000 times or TUNEL detect solution (Beyotime, Shanghai,

China) for 5 min, washed with PBS for 5 min three times, and observed under a fluorescence microscope (Leica Microsystems, Weitzlar, Germany).

#### *Cell Viability Assay*

Cells (100  $\mu$ L/well) were seed in 96-well plates and added 5 g/L 3-(4,5-dimethyl-2-thiazolyl)-2,5-diphenyl-2-H-tetrazoliumbromide (MTT) solution (Beyotime, Shanghai, China) for incubation at 37 °C for 4 h. After abandoning the supernatant, dimethyl sulfoxide (DMSO; Beyotime, Shanghai, China) was added to each well to dissolve the crystals fully for 30 min, and then the absorption values of each well at the wavelength of 490 nm (OD490) were tested by spectrophotometer (Aucy Instrument Inc., Shanghai, China).

#### *Statistical Analysis*

All data were statistically analyzed using SPSS 20.0 software (SPSS Inc., Chicago, USA) and presented as mean  $\pm$  standard deviation (SD) after homogeneity test. In addition, data between the two groups were compared by using student's *t* test, and  $p < 0.05$  was considered statistically significant.

## RESULTS

### *Cilostazol Promoted Angiogenesis, Decreased Infarct Area and Cardiomyocyte Apoptosis in Myocardial I/R-Injury Rat Model*

To observe the functional role of cilostazol in angiogenesis in I/R injury, myocardial tissues from I/R-injury rat model were observed using immunohistochemistry. The results suggested that I/R-injury decreased blood vessels and cilostazol significantly increased the numbers of new blood vessels myocardial tissues of I/R-injury rat model (Fig. 1a). Western blotting assay displayed that the protein expressions of VEGF, HGF, bFGF and PDGF-B were higher in sham + cilostazol group and I/R group than that in the sham group ( $p < 0.05$  and  $p < 0.01$ , respectively), and particularly, the highest expression levels were emerged in I/R + cilostazol group ( $p < 0.001$ , Fig. 1b). Similarly, qRT-PCR results in Fig. 1c showed that cilostazol significantly increased the expression levels of VEGF, HGF, bFGF and PDGF-B as compared to the sham or I/R group. Hence, these results illustrated that cilostazol could promote angiogenesis in myocardial I/R-injury rat model. Then, the TCC results significantly showed that the myocardial infarction area was increased in I/R group

and then cilostazol inhibited the increase of infarction area induced by I/R ( $p < 0.001$ , Fig. 1d). Further, HE results displayed that the morphological structure of cardiomyocytes in the sham and sham + cilostazol group were basically normal with interstitial hyperemia, but these cells were arranged; the cardiomyocytes in I/R group were disordered and the cells were degenerated; the cardiomyocytes in I/R + cilostazol group were arranged neatly with a small amount of degeneration and interstitial hyperemia, suggesting that cilostazol could repair myocardial cell injury induced by I/R (Fig. 1e). In Fig. 1f, TUNEL results showed that positive TUNEL cell number in I/R + cilostazol group was less than that in I/R group, suggesting that cilostazol inhibited cardiomyocyte apoptosis in I/R-injury rat model ( $p < 0.001$ ).

### *Cilostazol Increased Cell Proliferation in H/I Cell Models*

H/I HUVEC and VSMC cell models were established to explore the effects of cilostazol on I/R-injury *in vitro*. Comparing with the control group, western blotting showed that the expression level of p-AKT and p-eNOS were remarkably decreased in H/I group, but increased in cilostazol group ( $p < 0.01$  and  $p < 0.05$ , respectively). Indeed, cilostazol treatment attenuated the down-regulation of p-AKT and p-eNOS induced by H/I-injury ( $p < 0.001$ , Fig. 2a). Brdu staining displayed that cilostazol increased the number of positive cells in H/I HUVEC cells (Fig. 2a). Consistently, as shown in Fig. 2b, the enhancement of AKT and eNOS phosphorylation level and positive cell numbers were exhibited in VSMC cell model after cilostazol treatment ( $p < 0.01$  and  $p < 0.001$ , respectively). These investigations suggested that cilostazol could increase cell proliferation in H/I cell models *in vitro*.

### *Cilostazol Promoted Angiogenesis and Increased Cell Viability in a cAMP-Dependent Manner in H/I Cell Model*

Finally, we used 8-Br-cAMP (the analogues of cAMP) and KT-5720 (the antagonist of cAMP) to study the underlying mechanism underlying the influences of cilostazol in myocardial I/R injury. Figure 3a showed that apoptosis-related proteins cleaved-caspase 3 and cleaved-PARP were significantly decreased, and AKT phosphorylation level was increased in the H/I + cilostazol group as compared to the H/R group ( $p < 0.001$ ). After 8-Br-cAMP treatment, the expression level of VEGF, HGF, bFGF, PDGF-B, p-AKT and p-eNOS were up-regulated while the expression level of cleaved-caspase 3 and cleaved-PARP were

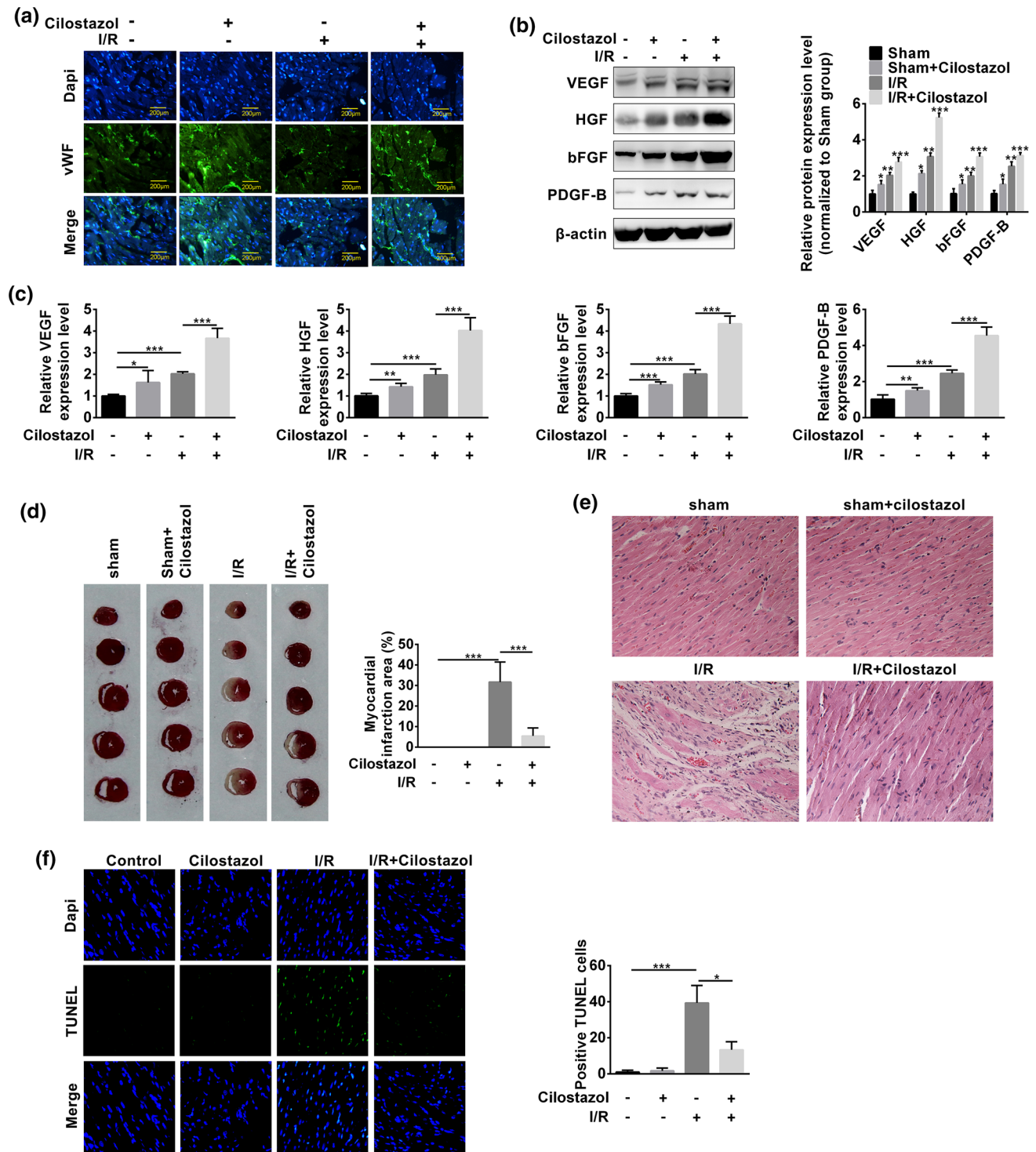


**FIGURE 1.** Effect of cilostazol on angiogenesis in myocardial tissues of I/R injure rat model. (a) Immunohistochemistry were used to detect the number of new blood vessel. (b) Western blotting and (c) qRT-PCR were used to test the mRNA and protein expression levels of VEGF, HGF, bFGF and PDGF-B in myocardial tissues of I/R injure rat model (n = 40). \*p < 0.05, \*\*p < 0.01 and \*\*\*p < 0.001.

down-regulated in H/I + cilostazol + 8-Br-cAMP group as compared to the H/I + cilostazol group (p < 0.01 and p < 0.001, respectively). The completely reversed results were observed in the

H/I + cilostazol + KT-5720 group (p < 0.01 and p < 0.001, respectively). Brdu staining results revealed that the number of positive cells in the H/I + cilostazol group was more than that in the

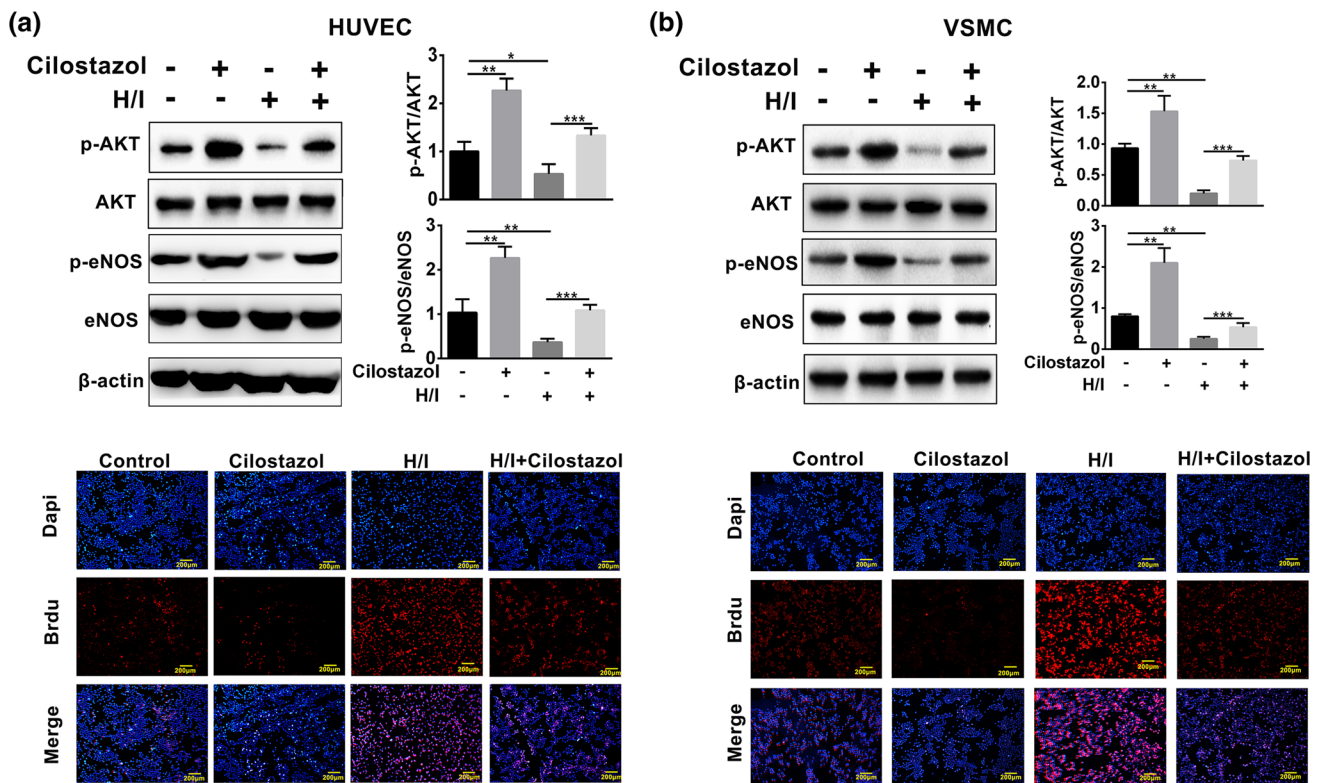


**FIGURE 2.** Cilostazol increased cell proliferation in H/I cell models. The protein expression levels of p-AKT and p-eNOS and proliferation in (a) HUVEC H/I cell model and (b) VSMC H/I cell model. The protein expression was detected by western blotting, and cell proliferation was analyzed by DAPI/Brdu staining. \* $p < 0.05$ , \*\* $p < 0.01$  and \*\*\* $p < 0.001$ .

H/I + cilostazol + KT-5720 group, and less than that in the H/I + cilostazol + 8-Br-cAMP group (Fig. 3b). Conversely, positive staining rate of TUNEL staining was reduced after 8-Br-cAMP treatment and increased by KT-5720 treatment (Fig. 3c). Besides, as shown in Fig. 3d, cell viability was decreased in H/I cell model compared with normal cells. Cilostazol clearly increased cell viability, which was aggravated by 8-Br-cAMP and attenuated after KT-5720 treatment, respectively ( $p < 0.001$ ). Totally, cilostazol promoted angiogenesis, increased cell viability, and inhibited apoptosis through activating cAMP in H/I cell model.

## DISCUSSION

Ischemia is well-known responsible for hypoxia and accumulation of metabolites, such as lactic acid, various inorganic salts, adenosine; and reperfusion, leading to oxidizing load and loss of cellular metabolites.<sup>9,22</sup> These abnormalities in turn cause the weakening of cardiac function, blockage of energy metabolism and damage of oxygen free radicals.<sup>9,22</sup> A previous study reported that the factors causing I/R injury are not only related to calcium overload and oxygen free radicals, but also associated with

endothelial cell homeostasis.<sup>36</sup> I/R gives rise to the impairment of endothelial cell function and the loss of the dynamic balance between prostaglandin I<sub>2</sub> (PGI<sub>2</sub>) and TXA<sub>2</sub>.<sup>38</sup> Therefore, in addition to constructing myocardial I/R rat model, we also used human vascular endothelial cells to simulate I/R injury *in vitro*.

Cilostazol, as a PDE3 inhibitor, has been shown to exert anti-thrombotic effects by inhibiting platelet aggregation.<sup>37</sup> Herath *et al.* suggested that cilostazol promotes angiogenesis in ischemic areas, which may be associated with the expression of angiotensin II, VEGF, bFGF and other pro-angiogenic factors.<sup>12</sup> Consistently, our study showed similar results that cilostazol accelerated angiogenesis in myocardial I/R rat model. Besides, VEGF and its receptors expressions are significantly multiplied during myocardial ischemia or hypoxia, suggesting that VEGF is closely related to myocardial I/R-injury.<sup>26</sup> It also has been reported that VEGF can promote vascular permeability, vascular endothelial cell migration, proliferation and angiogenesis.<sup>26</sup> HGF can promote and regulate cell growth, movement and angiogenesis in epithelial cells, hematopoietic cells and vascular endothelial cells.<sup>21</sup> Moreover, HGF plays an important effect on embryogenesis, wound healing, angiogenesis and carcinogenesis by the mechanisms of paracrine or autocrine and the

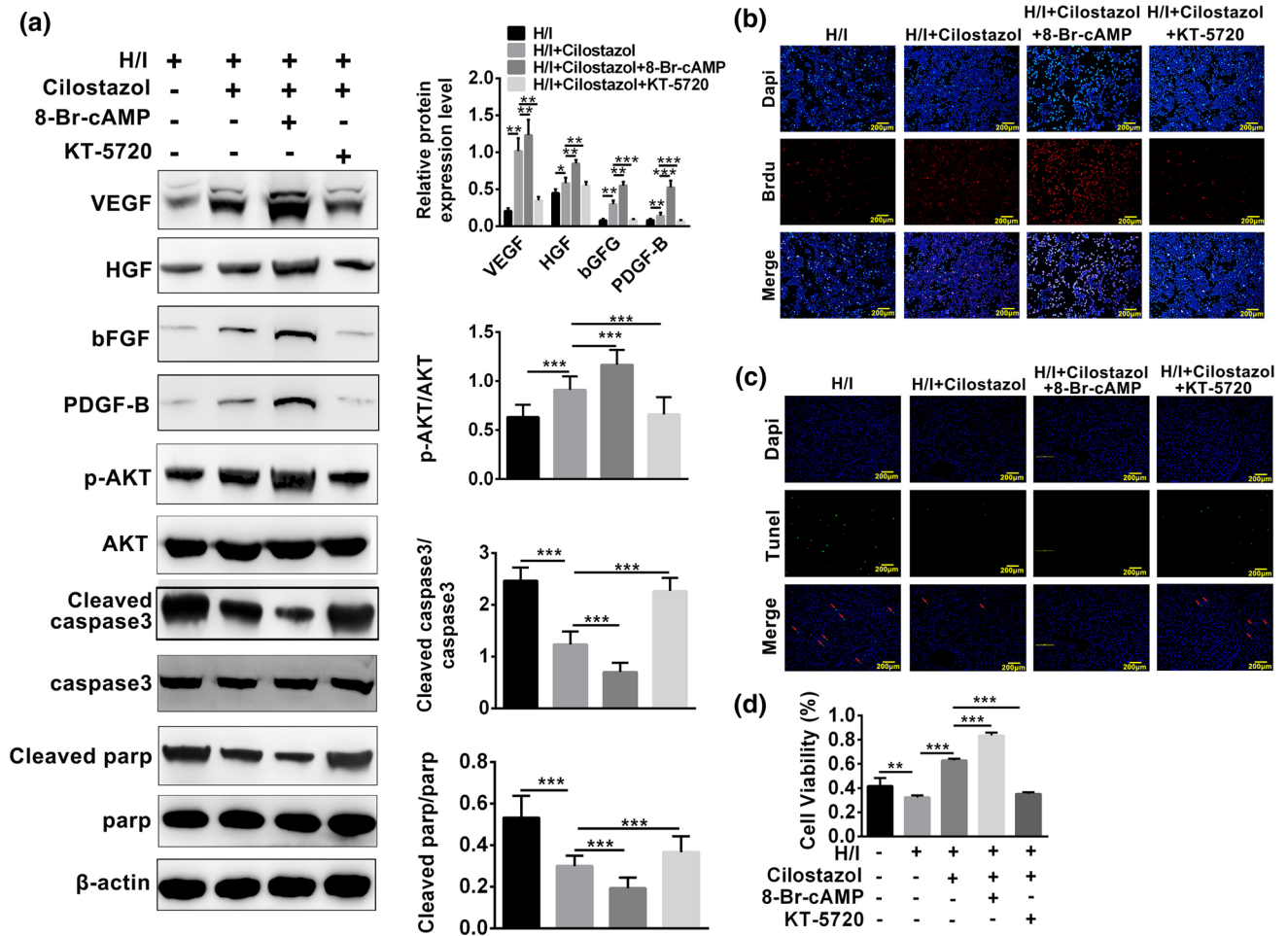


**FIGURE 3.** Cilostazol promoted angiogenesis and increased cell viability in a cAMP-dependent manner in H/I cell model. (a) Western blotting was used to measure the protein expression levels of VEGF, HGF, bFGF, PDGF-B, p-AKT, p-eNOS, cleaved-caspase 3 and cleaved-PARP. (b) Cell proliferation, (c) apoptosis and (d) cell viability were tested by DAPI/BrdU, DAPI/TUNEL staining and MTT assay, respectively. \* $p < 0.05$ , \*\* $p < 0.01$  and \*\*\* $p < 0.001$ .

interaction of epithelial and mesenchymal cells.<sup>21,29</sup> Then, cilostazol-induced angiogenesis has been shown to be VEGF-dependent or primarily relying on HGF in models of peripheral ischemia.<sup>4,30</sup> As a highly potent angiogenic stimulator, bFGF acts directly on smooth muscle cells and vascular endothelial cells.<sup>14</sup> *In vitro* experiments showed that the combined application of VEGF and bFGF could exert greater angiogenic influences.<sup>5</sup> Similarly, PDGF-B is a profile inducer of angiogenesis which up-regulates VEGF and bFGF expression, while vascular endothelial cells can express PDGF-B receptors and mediate PDGF-induced vascular regeneration.<sup>34</sup> Therefore, we selected these four factors to become our reference test indicators in the study. In our study, cilostazol increased VEGF, bFGF, PDGF-B and HGF expression levels in I/R injure rat model. In addition, we also found that cilostazol could promote angiogenesis, decrease infarct area and inhibit cardiomyocyte apoptosis in I/R injure rat model.

It has been confirmed that cilostazol alleviates I/R injury by elevating the phosphorylation level of eNOS to produce NO, adiponectin and blood flow velocity in peripheral area of the ischemic lesion.<sup>25,27</sup> Cilostazol also strengthens proliferation, NO production and angiogenesis of HUVEC cells in hind limb ischemia models through activating multiple signaling pathways downstream of PI3K/AKT/eNOS.<sup>6</sup> A report have found that endoplasmic reticulum stress (ERS)-related apoptotic pathways also participate in myocardial I/R injury.<sup>39</sup> Activation of PI3K/AKT pathway can regulate ERS response, reduce caspase-12 and chop expression, inhibit apoptosis and promote the increase of AKT phosphorylation in myocardium after I/R.<sup>39</sup> Hence, we also detected the phosphorylation level of eNOS and AKT in H/I cell models, and found that eNOS and AKT expression were up-regulated after cilostazol treatment, conjecturing that cilostazol might facilitate cell proliferation.

Furthermore, Liu *et al.* demonstrated that the inhibitory effect of cilostazol on cell proliferation may be connected to its ability to induce apoptosis: cilostazol stimulates cAMP accumulation *in vivo* by inhibiting PED3 activity, and further up-regulates the expressions of tumor suppressor genes P53, P21 and HGF, thereby inducing apoptosis and enhancing the anti-proliferation *via* regulating cell cycle.<sup>21</sup> However, several studies showed that cilostazol accelerates proliferation and inhibits apoptosis to protect against hind limb ischemic injury or promote hair growth.<sup>6,7</sup> In this study, we observed that cilostazol increased the positive cell number in H/I cell model. In addition, cilostazol down-regulated the protein levels of cleaved caspase-3 and PARP, as well as decreased positive staining of TUNEL. These results revealed that cilostazol could promote cell proliferation and prevent apoptosis in I/R injury.

Previous study indicated that the level of cAMP in vascular smooth muscle was elevated by cilostazol through blocking calcium release and inhibiting muscle contraction.<sup>19</sup> The hypolipidemic mechanism of cilostazol may be due to the enhancement of cAMP that reduces the secretion of very low density lipoprotein (VLDL) in mouse stem cells by activating the PKA pathway.<sup>28</sup> We speculated that activation of cAMP may be one of the mechanisms underlying the protective role of cilostazol in ischemic heart. In this experiment, the addition of 8-Br-cAMP aggrandized the promotion of proliferation or inhibition of apoptosis by cilostazol. On the contrary, PKA antagonist KT-5720 attenuated the effects of cilostazol. All data illustrated that cilostazol could protect myocardial tissue from I/R injury primarily through activation and regulation of the cAMP pathway.

## CONCLUSION

In short, cilostazol has a protective influence in myocardial I/R-injury, which may be related to activation of cAMP pathway to promote angiogenesis. Above data have potential clinical therapeutic implications for ischemic heart diseases. We still need to perform more detailed experiments to further explore the possible regulatory mechanisms of cilostazol in alleviating myocardial I/R-injury.

## COMPETING INTERESTS

The authors declare that they have no competing interests, and all authors should confirm its accuracy.

## REFERENCES

- Adnan, M., G. Morton, and S. Hadi. Analysis of rpoS and bolA gene expression under various stress-induced environments in planktonic and biofilm phase using 2(-DeltaDeltaCT) method. *Mol. Cell. Biochem.* 357(1–2):275–282, 2011. <https://doi.org/10.1007/s11010-011-0898-y>.
- Asal, N. J., and K. A. Wojciak. Effect of cilostazol in treating diabetes-associated microvascular complications. *Endocrine* 56(2):240–244, 2017. <https://doi.org/10.1007/s12020-017-1279-4>.
- Ba, X. H., L. P. Cai, and W. Han. Effect of cilostazol pretreatment on the PARP/AIF-mediated apoptotic pathway in rat cerebral ischemia-reperfusion models. *Exp. Ther. Med.* 7(5):1209–1214, 2014. <https://doi.org/10.3892/etm.2014.1551>.
- Biscetti, F., G. Pecorini, G. Straface, V. Arena, E. Stigliano, S. Rutella, F. Locatelli, F. Angelini, G. Ghirlanda, and A. Flex. Cilostazol promotes angiogenesis after peripheral ischemia through a VEGF-dependent mechanism. *Int. J. Cardiol.* 167(3):910–916, 2013. <https://doi.org/10.1016/j.ijcard.2012.03.103>.
- Brogi, E., T. Wu, A. Namiki, and J. M. Isner. Indirect angiogenic cytokines upregulate VEGF and bFGF gene expression in vascular smooth muscle cells, whereas hypoxia upregulates VEGF expression only. *Circulation* 90(2):649–652, 1994.
- Chao, T. H., S. Y. Tseng, Y. H. Li, P. Y. Liu, C. L. Cho, G. Y. Shi, H. L. Wu, and J. H. Chen. A novel vasculo-angiogenic effect of cilostazol mediated by cross-talk between multiple signalling pathways including the ERK/p38 MAPK signalling transduction cascade. *Clin. Sci. (Lond.)* 123(3):147–159, 2012. <https://doi.org/10.1042/cs20110432>.
- Choi, H. I., D. Y. Kim, S. J. Choi, C. Y. Shin, S. T. Hwang, K. H. Kim, and O. Kwon. The effect of cilostazol, a phosphodiesterase 3 (PDE3) inhibitor, on human hair growth with the dual promoting mechanisms. *J. Dermatol. Sci.* 91(1):60–68, 2018. <https://doi.org/10.1016/j.jdermsci.2018.04.005>.
- Collaboration, H. S. Homocysteine and risk of ischemic heart disease and stroke: a meta-analysis. *JAMA* 288(16):2015–2022, 2002.
- Eltzschig, H. K., and T. Eckle. Ischemia and reperfusion—from mechanism to translation. *Nat. Med.* 17(11):1391–1401, 2011. <https://doi.org/10.1038/nm.2507>.
- Frias Neto, C. A., M. K. Koike, K. R. Saad, P. F. Saad, and E. F. Montero. Effects of ischemic preconditioning and cilostazol on muscle ischemia-reperfusion injury in rats. *Acta Cir Bras.* 29(Suppl 3):17–21, 2014.
- Hayward, C. P., K. A. Moffat, J. F. Castilloux, Y. Liu, J. Seecharan, S. Tasneem, S. Carlino, A. Cormier, and G. E. Rivard. Simultaneous measurement of adenosine triphosphate release and aggregation potentiates human platelet aggregation responses for some subjects, including persons with Quebec platelet disorder. *Thromb. Haemost.* 107(4):726–734, 2012. <https://doi.org/10.1160/th11-10-0740>.
- Herath, S. C., T. Lion, M. Klein, D. Stenger, C. Scheuer, J. H. Holstein, P. Morsdorf, M. F. Rollmann, T. Pohlemann, M. D. Menger, *et al.* Stimulation of angiogenesis by cilostazol accelerates fracture healing in mice. *J. Orthop. Res.* 33(12):1880–1887, 2015. <https://doi.org/10.1002/jor.22967>.
- Hol, P. K., P. S. Lingaas, R. Lundblad, K. A. Rein, K. Vatne, H. J. Smith, S. Nitter-Hauge, and E. Fosse. Intra-

- operative angiography leads to graft revision in coronary artery bypass surgery. *Ann. Thorac. Surg.* 78(2):502–505, 2004; discussion 505. <https://doi.org/10.1016/j.athoracsur.2004.03.004>.
- <sup>14</sup>Hu, M., Y. Hu, J. He, and B. Li. Prognostic value of basic fibroblast growth factor (bFGF) in lung cancer: a systematic review with meta-analysis. *PLoS ONE* 11(1):e0147374, 2016. <https://doi.org/10.1371/journal.pone.0147374>.
- <sup>15</sup>Huang, Y., Y. Cheng, J. Wu, Y. Li, E. Xu, Z. Hong, Z. Li, W. Zhang, M. Ding, X. Gao, et al. Cilostazol as an alternative to aspirin after ischaemic stroke: a randomised, double-blind, pilot study. *Lancet Neurol.* 7(6):494–499, 2008. [https://doi.org/10.1016/s1474-4422\(08\)70094-2](https://doi.org/10.1016/s1474-4422(08)70094-2).
- <sup>16</sup>Huang, J. H., X. H. Huang, Z. Y. Chen, Q. S. Zheng, and R. Y. Sun. Equivalent dose conversion between animals and between animals and humans in pharmacological tests (In Chinese). *Chin. J. Clin. Pharmacol. Ther.* 9(9):1069–1072, 2004.
- <sup>17</sup>Jeon, C., S. C. Candia, J. C. Wang, E. M. Holper, M. Ammerer, R. E. Kuntz, and L. Mauri. Relative spatial distributions of coronary artery bypass graft insertion and acute thrombosis: a model for protection from acute myocardial infarction. *Am. Heart J.* 160(1):195–201, 2010. <https://doi.org/10.1016/j.ahj.2010.04.004>.
- <sup>18</sup>Kariyazono, H., K. Nakamura, T. Shinkawa, T. Yamaguchi, R. Sakata, and K. Yamada. Inhibition of platelet aggregation and the release of P-selectin from platelets by cilostazol. *Thromb. Res.* 101(6):445–453, 2001.
- <sup>19</sup>Li, H., D. H. Hong, Y. K. Son, S. H. Na, W. K. Jung, Y. M. Bae, E. Y. Seo, S. J. Kim, I. W. Choi, and W. S. Park. Cilostazol induces vasodilation through the activation of Ca(2+)-activated K(+) channels in aortic smooth muscle. *Vascul. Pharmacol.* 70:15–22, 2015. <https://doi.org/10.1016/j.vph.2015.01.002>.
- <sup>20</sup>Li, J., X. Xiang, X. Gong, Y. Shi, J. Yang, and Z. Xu. Cilostazol protects mice against myocardium ischemic/reperfusion injury by activating a PPARgamma/JAK2/STAT3 pathway. *Biomed. Pharmacother.* 94:995–1001, 2017. <https://doi.org/10.1016/j.biopha.2017.07.143>; (PMID: 28810537).
- <sup>21</sup>Liu, Y., T. Wang, J. Yan, N. Jiabogou, D. A. Heideman, A. E. Canfield, and M. Y. Alexander. HGF/c-Met signalling promotes Notch3 activation and human vascular smooth muscle cell osteogenic differentiation in vitro. *Atherosclerosis* 219(2):440–447, 2011. <https://doi.org/10.1016/j.atherosclerosis.2011.08.033>.
- <sup>22</sup>Matsui, Y., H. Takagi, X. Qu, M. Abdellatif, H. Sakoda, T. Asano, B. Levine, and J. Sadoshima. Distinct roles of autophagy in the heart during ischemia and reperfusion: roles of AMP-activated protein kinase and Beclin 1 in mediating autophagy. *Circ. Res.* 100(6):914–922, 2007. <https://doi.org/10.1161/01.res.0000261924.76669.36>.
- <sup>23</sup>Mazur, C., K. Mullane, and M. A. Young. Acadesine preserves cardiac function and enhances coronary blood flow in isolated, blood perfused rabbit hearts with repeated ischemia and reperfusion. *J. Mol. Cell. Cardiol.* 23:S45, 1991. [https://doi.org/10.1016/0022-2828\(91\)91458-4](https://doi.org/10.1016/0022-2828(91)91458-4).
- <sup>24</sup>Murphy, E., and C. Steenbergen. Mechanisms underlying acute protection from cardiac ischemia-reperfusion injury. *Physiol. Rev.* 88(2):581–609, 2008. <https://doi.org/10.1152/physrev.00024.2007>.
- <sup>25</sup>Oyama, N., Y. Yagita, M. Kawamura, Y. Sugiyama, Y. Terasaki, E. Omura-Matsuoka, T. Sasaki, and K. Kitagawa. Cilostazol, not aspirin, reduces ischemic brain injury via endothelial protection in spontaneously hypertensive rats. *Stroke* 42(9):2571–2577, 2011. <https://doi.org/10.1161/strokeaha.110.609834>.
- <sup>26</sup>Peters, T. H., V. Sharma, E. Yilmaz, W. J. Mooi, A. J. Bogers, and H. S. Sharma. DNA microarray and quantitative analysis reveal enhanced myocardial VEGF expression with stunted angiogenesis in human tetralogy of Fallot. *Cell Biochem. Biophys.* 67(2):305–316, 2013. <https://doi.org/10.1007/s12013-013-9710-9>.
- <sup>27</sup>Ragab, D., D. M. Abdallah, and H. S. El-Abhar. Cilostazol renoprotective effect: modulation of PPAR-gamma, NGAL, KIM-1 and IL-18 underlies its novel effect in a model of ischemia-reperfusion. *PLoS ONE* 9(5):e95313, 2014. <https://doi.org/10.1371/journal.pone.0095313>.
- <sup>28</sup>Rizzo, M., E. Corrado, A. M. Patti, G. B. Rini, and D. P. Mikhailidis. Cilostazol and atherogenic dyslipidemia: a clinically relevant effect? *Expert Opin. Pharmacother.* 12(4):647–655, 2011. <https://doi.org/10.1517/14656566.2011.557359>.
- <sup>29</sup>Rosen, E. M., K. Lamszus, J. Laterra, P. J. Polverini, J. S. Rubin, and I. D. Goldberg. HGF/SF in angiogenesis. *Ciba Found. Symp.* 212:215–226; discussion 227–219, 1997.
- <sup>30</sup>Sanada, F., Y. Kanbara, Y. Taniyama, R. Otsu, M. Caracado, Y. Ikeda-Iwabu, J. Muratsu, K. Sugimoto, K. Yamamoto, H. Rakugi, et al. Induction of angiogenesis by a type III phosphodiesterase inhibitor, cilostazol, through activation of peroxisome proliferator-activated receptor-gamma and cAMP pathways in vascular cells. *Arterioscler. Thromb. Vasc. Biol.* 36(3):545–552, 2016. <https://doi.org/10.1161/atvbaha.115.307011>.
- <sup>31</sup>Shimizu, T., T. Osumi, K. Niimi, and K. Nakagawa. Physico-chemical properties and stability of cilostazol. *Arzneimittelforschung* 35(7a):1117–1123, 1985.
- <sup>32</sup>Tanaka, H., N. Zaima, H. Ito, K. Hattori, N. Yamamoto, H. Konno, M. Setou, and N. Unno. Cilostazol inhibits accumulation of triglycerides in a rat model of carotid artery ligation. *J. Vasc. Surg.* 58(5):1366–1374, 2013. <https://doi.org/10.1016/j.jvs.2013.01.033>.
- <sup>33</sup>von Heesen, M., S. Muller, U. Keppler, M. J. Strowitzki, C. Scheuer, M. K. Schilling, M. D. Menger, and M. R. Moussavian. Preconditioning by cilostazol protects against cold hepatic ischemia-reperfusion injury. *Ann Transplant.* 20:160–168, 2015. <https://doi.org/10.12659/aot.893031>.
- <sup>34</sup>Wang, X. T., P. Y. Liu, and J. B. Tang. PDGF gene therapy enhances expression of VEGF and bFGF genes and activates the NF-kappaB gene in signal pathways in ischemic flaps. *Plast. Reconstr. Surg.* 117(1):129–137; discussion 138–129, 2006.
- <sup>35</sup>Wang, C., C. Wang, Q. Liu, Q. Meng, J. Cang, H. Sun, J. Peng, X. Ma, X. Huo, and K. Liu. Aspirin and probenecid inhibit organic anion transporter 3-mediated renal uptake of cilostazol and probenecid induces metabolism of cilostazol in the rat. *Drug Metab. Dispos.* 42(6):996–1007, 2014. <https://doi.org/10.1124/dmd.113.055194>.
- <sup>36</sup>Wu, D., J. Wang, H. Li, M. Xue, A. Ji, and Y. Li. Role of hydrogen sulfide in ischemia-reperfusion injury. *Oxid. Med. Cell Longev.* 2015:186908, 2015. <https://doi.org/10.1155/2015/186908>.
- <sup>37</sup>Yamamoto, S., R. Kurokawa, and P. Kim. Cilostazol, a selective Type III phosphodiesterase inhibitor: prevention of cervical myelopathy in a rat chronic compression model. *J. Neurosurg. Spine* 20(1):93–101, 2014. <https://doi.org/10.3171/2013.9.spine.121136>.
- <sup>38</sup>Yu, L., B. Yang, J. Wang, L. Zhao, W. Luo, Q. Jiang, and J. Yang. Time course change of COX2-PGI2/TXA2 following global cerebral ischemia reperfusion injury in rat

hippocampus. *Behav. Brain Funct.* 10:42, 2014. <https://doi.org/10.1186/1744-9081-10-42>.

<sup>39</sup>Zhang, G. G., X. Teng, Y. Liu, Y. Cai, Y. B. Zhou, X. H. Duan, J. Q. Song, Y. Shi, C. S. Tang, X. H. Yin, *et al.* Inhibition of endoplasm reticulum stress by ghrelin protects against ischemia/reperfusion injury in rat heart. *Peptides*

30(6):1109–1116, 2009. <https://doi.org/10.1016/j.peptides.2009.03.024>.

**Publisher's Note** Springer Nature remains neutral with regard to jurisdictional claims in published maps and institutional affiliations.